10-20-2005

Acoustic Waves Generated by Gusty Flow over Hilly Terrain

R. L. Walterscheid
The Aerospace Corporation

Michael P. Hickey Ph.D.
Embry-Riddle Aeronautical University, hicke0b5@erau.edu

Walterscheid, R. L., and M. P. Hickey (2005), Acoustic waves generated by gusty flow over hilly terrain, J. Geophys. Res., 110, A10307, doi: https://doi.org/10.1029/2005JA011166

Acoustic waves generated by gusty flow over hilly terrain

R. L. Walterscheid[1]
The Aerospace Corporation, Los Angeles, California, USA

M. P. Hickey[2]
Department of Physical Sciences, Embry Riddle Aeronautical University, Daytona Beach, Florida, USA

Received 3 April 2005; revised 27 May 2005; accepted 28 June 2005; published 20 October 2005.

[1] We examine the generation of acoustic waves by gusty flow over hilly terrain. We use simple theoretical models of the interaction between terrain and eddies and a linear model of acoustic-gravity wave propagation. The calculations presented here suggest that over a dense array of geographically extensive sources orographically generated vertically propagating acoustic waves can be a significant cause of thermospheric heating. This heating may account in good part for the thermospheric hot spot near the Andes reported by Meriwether et al. (1996, 1997).

Citation: Walterscheid, R. L., and M. P. Hickey (2005), Acoustic waves generated by gusty flow over hilly terrain, *J. Geophys. Res.*, *110*, A10307, doi:10.1029/2005JA011166.

1. Introduction

[2] Observations and modeling indicate that variable flow over terrain is a likely source of high-frequency waves in the upper mesosphere and lower thermosphere (MLT). There is accumulating evidence of enhanced power near the Brunt-Väisälä frequency. A recent analysis of OH airglow data from an instrument sited in Boulder, Colorado indicates persistent elevated power near the Brunt- Väisälä frequency over a 56 day period [*Sivjee and Walterscheid*, 2005]. The persistence of the feature and its nighttime occurrence together suggest that the enhancement is attributable to the proximity of the Rocky Mountains. Nighttime convection was not a plausible source of such a persistent enhancement. Similar evidence of elevated power near the Brunt- Väisälä frequency was seen in radar observations at Jicamarca Radar Observatory near the Peruvian Andes [*Rastogi and Bowhill*, 1976]. *Hocke and Tsuda* [2001] found centers of enhanced ion density variance in Global Positioning System occultation data up- and downwind of the Andes and identified the Andes as the source of the waves. The upwind waves could only be generated by unsteady flow.

[3] The most important effects of acoustic waves are expected in the thermosphere. These waves can propagate to great heights with minimal dissipation [*Walterscheid et al.*, 2003; *Jones*, 1970; *Raju et al.*, 1981; *Rind*, 1978]. Internal acoustic waves can reach much greater altitudes than internal gravity waves with the same vertical scale (same scale-dependent dissipation rate). Thus waves with insensible amplitudes at the ground can propagate high in the thermosphere where they can achieve significant amplitudes and produce large effects. This is accentuated by the fact that acoustic waves, being high-frequency waves, deliver more power to the thermosphere than gravity waves of the same amplitude.

[4] There is circumstantial evidence of high-frequency waves in the thermosphere originating from terrain. Wave heating of the thermosphere is suggested by observations of enhanced temperature variability in connection with the hot spot observed by *Meriwether et al.* [1996, 1997] in the OI 630 nm redline airglow near the Andes. The redline airglow originates from a thick layer nominally peaking ~250 km [*Solomon and Abreu*, 1989; *Takahashi et al.*, 1990]. If wave heating is the cause of the hot spots, the waves must be fast waves to survive dissipation in the viscous lower thermosphere. The simulation of waves generated by flow over terrain has shown that the transients due to orographic generation may be the source of waves for the MLT [*Prusa et al.*, 1996].

[5] Orographic sources for waves near the Brunt-Vaisala frequency, or waves fast enough to reach redline altitudes, do not necessarily imply significant orographic generation of acoustic waves. However, such generation seems reasonable since the gust and eddy spectrum has significant power at acoustic frequencies, especially over rough terrain. The energy in the gust spectrum peaks in the acoustic range [*Van der Hoven*, 1957] with peak gust power near 1–2 min periods. The power in the gust part of the spectrum varies with wind speed and can be quite significant. For moderately strong winds of ~10 m s^{-1}, gusts amplitudes are $u \sim 4$ m s^{-1} at 10 m above rough terrain (roughness length ~1 m) [*Lumley and Panofsky*, 1964, equation (4.25)].

[6] An enhancement of high-frequency waves in the acoustic range is seen in the spectrum of highly time-resolved airglow data from the Starfire Optical Range (J. H. Hecht, personal communication, 2002). Power spectra of OH Meinel brightness for two time segments for the night of 17 November 1999 show a flattening of the spectrum with

[1] Currently at NOAA European Organisation for the Exploitation of Meteorological Satellites (EUMATSAT), Darmstadt, Germany.
[2] Also at the Aerospace Corporation, Los Angeles, California, USA.

0148-0227/05/2005JA011166

elevated power at high gravity-wave frequencies and elevated power extending to frequencies above the Brunt-Väisälä frequency, with significant power well into the internal acoustic regime. The noise floor commenced around 45 s. It is not likely that convection is the source of this elevated power, as there was no plausible convective source when the data were taken. The Starfire Optical Range is located in a mountainous region and orographic generation seems likely. Similar evidence of elevated power in the acoustic range was seen at the high-altitude observatory at Haleakala [*Hecht et al.*, 1995].

[7] For equal source amplitudes, the acoustic waves that are most likely to have significant amplitudes in the MLT are those that propagate nearly vertically (those with horizontal wave number $k \approx 0$). These waves are less subject to attenuation by evanescence, since they are vertically propagating over a greater range of frequencies (all frequencies above the acoustic cutoff frequency). As k increases, the boundary between vertical propagation and evanescence occurs at ever increasing frequency. Also, $k \approx 0$ waves do not suffer viscous attenuation because of horizontal gradients and are insensitive to background winds. Finally, there is very little horizontal spreading of a wave packet as it propagates vertically. This has particular significance for isolated hills, since there is little attenuation of the wave due to geometric spreading.

[8] Acoustic waves may be generated by rapid variations in convection (dry and moist), instabilities, and small-scale turbulence. Convecting eddies can generate acoustic waves through warming and cooling in up- and downdrafts. All forms of eddies may generate acoustic waves through the mechanical action of vertical motion and through the forced ascent and descent of air along sloping terrain. We dwell on the effects of motion constrained to move along sloping terrain and comment that the effects of convecting air may also be a significant source of acoustic energy. We comment on this further in the concluding section.

[9] For a symmetric hill, waves with $k \approx 0$ are generated by flow along sloping terrain by the part of the horizontal wind field that is antisymmetric with respect to the summits. For significant interactions between gusts and hills to occur there must be sufficient organization (coherency) and transience in the gust or eddy field over the dimension of the hill. As we shall see, very little amplitude is required to produce significant effects in the thermosphere.

[10] The required organization can come from small-scale gusts that are organized by larger scale eddies (or cells), or, as seems more likely, from the larger eddies themselves, provided they vary sufficiently rapidly. The variability can come from rapid changes in eddy strength and size as a result of the complex interplay of convection, shear, and gravity waves [*Redelsperger and Clark*, 1990].

[11] Large asymmetric eddies can originate in the asymmetric distribution of heating, shear driven instabilities, gravity wave generation, and nonlinear phenomena originating in boundary layer flow over obstacles (such as lulls, wakes, lee-side flow separation, and bubble formation) [*Redelsperger and Clark*, 1990; *Carruthers and Hunt*, 1990]. Some of the streamlines may approach the surface of the hill in the accelerating flow over hills, while others may recirculate in wake regions [*Belcher and Hunt*, 1998]. Causes of cellular structure occur when the hill is steep enough to cause separation [*Belcher and Hunt*, 1998]. Steep windward slopes can induce flow separation upwind of crests, while for a typically rounded hill, separation tends to occur in the lee about halfway down [*Barndorff-Nielson and Willetts*, 1991; *Taylor and Teunissen*, 1987].

[12] Calculations and observation for a case of neutral flow over an isolated hill indicate that the maximum wind is downwind of the summit and that regions of reverse flow exist [*Mason and Sykes*, 1979; *Carruthers and Hunt*, 1990; *Gopalakrishnan et al.*, 2000]. *Gopalakrishnan et al.* [2000] performed large eddy simulations (LESs) and found that the strongest and best organized eddies (hill lengths of $\sim$5 km) are highly asymmetric with the maximum vertical wind occurring near the summit. The asymmetry still exists for narrower and wider hills, but for the former it is less pronounced and weaker, and for the latter it is highly asymmetric and strong, but less well-organized. The strongest eddies were for lengths of $\sim$5 km and heights of 400 m (taller hills were not considered). *Allen and Brown* [2002] performed LES simulations with a model scaled to compare with wind tunnel data. The flow was over terrain that was steep enough to cause separation and the creation of a bubble in the lee.

[13] A high degree of transience can occur in boundary layer processes owing to boundary layer nonlinearities in flow over the hills, convection, gravity waves, and their interplay. The boundary layer may be distorted over horizontal length scales that are comparable to or less than the depth of the boundary layer so that a large fraction of the vertical extent of the boundary layer does not have time to come into equilibrium. Instabilities that give rise to eddies with scales of hundreds of meters can have very rapid growth rates ($\sim$ tens of seconds) [*Grabowski and Clark*, 1991]. In the simulations of *Allen and Brown* [2002], the length of the bubble changed rapidly, growing by 20% and shrinking by 10% of its mean length. Changes of this size occurred over $\sim$1/2 of an eddy turnover time. Scaled to the atmosphere this gives a timescale of $\sim$10 min [*Agee and Gluhovsky*, 1999].

[14] *Tian and Parker* [2003] simulated the diurnal variation in convection and gravity wave generation and the interplay of waves and eddies (including resonant interactions) over hills under various wind conditions. For a motionless background the flow is a vortex pair with one over each slope, giving a distribution for the along slope wind that is antisymmetric about the summit. The convergence at the summit associated with this distribution is a convective source of vertical wind that is in addition to that induced by the along slope horizontal wind. Under light wind conditions a large asymmetry remains, especially in the morning hours when downslope winds cause a large downward displacement of potential temperature surfaces. Stronger winds (10 m s^{-1}) cause significant orographic modification of convection by gravity waves. However, the greatest variability seems to be associated with weaker (2 m s^{-1}) winds, the height of the convective boundary layer (CBL) varies widely on short timescales, showing $\sim$100–300 m fluctuations over 30 min (the resolution of the plots). The convection dominated daytime average of the CBL height was $\sim$500 m.

[15] The existence of significant $k \approx 0$ acoustic power generated by gusty flow over hilly terrain is somewhat

conjectural. Sufficiently detailed field studies of the wind field over hills in the spatial and temporal domains simultaneously apparently do not exist. However, even weak interactions can produce significant effects in the thermosphere and models indicate that rapid variations can occur with the appropriate symmetries and scales; thus significant terrain generation of acoustic wave is at least plausible. In the following sections we discus some theoretical consideration, describe our wave model and calculations, present the results, and conclude with a discussion of the results and their significance.

2. Theory

[16] The terrain forcing of waves is given by

$$w = \mathbf{u} \cdot \nabla h, \tag{1}$$

where $\mathbf{u}$ is the horizontal velocity and w is the vertical velocity. For plane geometry

$$w = u\partial h/\partial x + v\partial h/\partial y, \tag{2}$$

where x and y are the horizontal coordinates and u and v are the respective velocity components ($\mathbf{u} = (u, v)$). For simplicity we consider two-dimensional flow over a ridge, whence $w = u\partial h/\partial x$. The forcing in a narrow band $k \in [-k_0, k_0]$ near $k = 0$ subject to $k_0 a \ll 1$, where a is the half width of the hill, is given approximately by

$$w_{\delta k} = -\frac{k_0}{\pi} \int_{-\infty}^{\infty} u(x) \frac{\partial h(x)}{\partial x} dx. \tag{3}$$

[17] We let the hill have a Gaussian shape and the antisymmetric eddy have a sinusoidal dependence about the center of the hill, thus

$$h = h_0 \exp\left[-(x/a)^2\right], u_{as} = U_{as}(t) \sin(\pi x/2a) S(x), \tag{4}$$

where $S(x) = 1$ if $x \in [-2a, 2a]$ and is zero otherwise. For present purposes it is sufficient to set $S(x) = 1$ for all x. Then approximately

$$\hat{w}_{\delta k} = \frac{\pi^{1/2}}{4} e^{-\pi^2/16} (h_0/l_0) U_{as} = 0.239 (h_0/l_0) U_{as}, \tag{5}$$

where l_0 is the length scale associated with k_0 (i.e., $l_0 = 1/k_0$) [*Gradshteyn and Ryzhik*, 1965, equation (3.952(1))].

[18] The parameter l_0 is evaluated as follows: we are interested in those acoustic waves with horizontal group speed u_g near zero. For $m \geq 0$, where m is the vertical wave number, the group speed is given by the slope of curves of constant m in the ω, k domain. At $k = 0$ these curves are flat (independent of k) with zero slope. As k increases, the curves remain nearly flat for a while and then turn up with the slope increasing until the slope begins to approach the sound speed (c_s). We take k_0 to be the value of k where the horizontal group speed is still very small (10 m s^{-1}, say) compared to the vertical group speed. Using Figure 3 from *Walterscheid and Hecht* [2003] gives a value of $k_0 \sim$ 1/30 km ($l_0 \sim$ 30 km). Thus terrain half-widths are restricted to $a \sim$ 10 km or less.

[19] For convenience we rewrite (5) in terms of the slope h_0/a as

$$\hat{w}_{\delta k} = 0.239 (h_0/a)(a/l_0) U_{as}.$$

Most hilly terrain is included in range of slopes between ~0.1 and 0.3, and in mountainous regions, slopes exceeding 35% can be found [*Gopalakrishnan et al.*, 2000]. The strongest and best organized eddies seem to be associated with hills with $a \sim$ 3 km. Thus $w_{\delta k} \sim 10^{-2} U_{as}$ seems reasonable.

[20] The next step is to evaluate the acoustic content of the eddy. Significant acoustic content can come from eddies whose life cycles are not too large compared to the acoustic cutoff period (~5 min in the troposphere). Significant acoustic content can also come from eddies originating from instabilities with rapid growth rates or from rapid changes in the eddy strength resulting from the complex interplay of convention, instabilities, and gravity waves.

[21] We assume an eddy of the temporal form

$$U_{as}(t) = U_o \cos(\omega_G t) S_G(t) \equiv U_o f(t), \tag{6}$$

where $\omega_G = \pi t_G^{-1}$ and $S_G(t) = 1$ for $t \in [-t_G/2, t_G/2]$ and is zero otherwise. Thus (6) represents an eddy that grows and decays with the same sign throughout. We are interested in resolving the spectral content of the disturbance into acoustic disturbances of various periods. To do this, we assume a basis of the form

$$\hat{g}_{\pm n}(\omega) = \frac{\sin[(\omega \pm n\omega_0) t_0/2]}{(\omega \pm n\omega_0) t_0/2}. \tag{7}$$

Functions of this form are analogous to the functions that serve as a basis for bandlimited functions. In the present case the function is time-limited and (7) serves as a basis for the spectrum. The projection of f on (7) is found by multiplying (7) by the value of the spectrum of f ($\hat{f}$) evaluated at $\omega_n = 2n\pi/t_0$ and taking the inverse transform. This gives disturbances of the form

$$f_n(t) = \hat{f}(n\omega_0) t_0^{-1} \cos(n\omega_0 t) S_O(t) \tag{8}$$

in the time domain, where $\omega_0 = 2\pi/t_0$ and $S_0(t) = 1$ for $t \in [-t_0/2, t_0/2]$ and is zero otherwise. This is the form of a localized wave packet with central frequency and bandwidth $n\omega_0$. The transform of f is

$$\hat{f}(\omega) = \frac{2\omega_0}{\omega_0^2 - \omega^2} \cos(\omega t_G/2). \tag{9}$$

By construction, $t_0 = t_G$ and $\omega_0 = 2\omega_G$, whence for $\pm n$

$$f_n(t) = \frac{4}{\pi} \frac{1}{1 - n^2} \cos(n\pi/2) \cos(n\omega_0 t) S_0(t) \equiv A_n \cos(n\omega_0 t) S_0(t) \tag{10}$$

[22] Table 1 gives the absolute values of A_n for various values of $n \geq 1$ for which A_n is nonzero ($n = 1$, and n even

Table 1. Amplitude of Wave Packets Compared With Eddy Amplitude for Various Values of n, Where Wave Frequency $\omega = 2\pi n/t_G$ and t_G is Gust Duration[a]

n	A_n
1	0.64
2	0.42
4	0.085
6	0.036
8	0.020
10	0.013

[a]For reference $n = 1$ refers to a 5 min wave when the gust duration is 10 min.

for $n > 1$). For reference, a gust duration of 10 min corresponds to a wave packet with a central frequency of 5 min when $n = 1$.

[23] It is much easier to generate a wave with given amplitude from an eddy with the form of a full cycle (e.g., the form of f) than from an eddy with the form of simple growth and decay. This is because an eddy with the form of a full cycle of duration t_G has its power concentrated at ω_G where $\omega_G = 2\pi/t_G$. For the same eddy duration, the wave amplitude generated at frequency ω_G from an eddy having the form of a full cycle is about twice that generated from a half cycle.

[24] Acoustic waves can also be generated by changes that rapidly take the wind strength from one level to another. Approximately time-limited changes of the form $f = H(1 - e^{-t/t_G})$, where H is the Heaviside step function, give $A_n \sim n^{-1}(1 + n^2)^{-1/2}$, where $n = 1$ if $t_n = t_G$. For a 10-min gust and a 5-min wave $A_2 = 0.22$. Thus changes of this type generate less acoustic energy than eddies that have a life cycle of growth and decay (see Table 1), but the difference is not huge. It does not appear too difficult for changes taking place over tens of minutes to generate acoustic power with ~1% efficiency or greater.

[25] The results shown in Table 1 indicate that acoustic frequency waves can be formed from ~10-min eddies with efficiencies A_n of ~0.1 down to wave periods of a few minutes. It does not seem likely that significant power could be realized for subminute waves.

[26] These results combined with the results above indicate that it might not be too difficult to force acoustic-frequency disturbances with vertical velocity amplitudes $w_{\delta k} \sim 10^{-3}\ U_{as}$. Thus amplitudes of U_{as} as small as 10^{-1} m s^{-1} could generate forcing amplitudes $w_{\delta k} \sim 10^{-4}$ m s^{-1}. Such small velocities are still significant, as the results given below indicate.

3. Wave Model and Calculations

[27] The upward propagation of acoustic waves is calculated with a full-wave model that solves the complete linearized equations of continuity, momentum, and energy for a compressible, viscous, and thermally conducting atmosphere with arbitrary altitude variations in basic state thermal structure. Unlike WKB models, the full-wave model rigorously accounts for wave reflection. Details of the model can be found in the works of *Hickey et al.* [2000, 2001] and *Schubert et al.* [2003, 2005]. The model domain extends from 1 km below the surface to an altitude of 600 km. The model vertical resolution is 2.4 m. A sponge layer at the top of the model domain insures against spurious wave reflections from the upper boundary. The sponge layer is implemented by assigning Rayleigh friction and Newtonian cooling coefficients that have the value of the wave frequency at the top of the model domain and decay exponentially downward with an e-folding length of 40 km.

[28] The boundary condition at the model lower boundary is more complicated. We solve the linearized equations of motion as a system of equations. This entails boundary conditions for each variable and a scheme to insure dynamical consistency between them. The model lower boundary condition is solved as a system subject to $w' = 0$. This was a very significant simplification and gave solutions free of artifacts. Implementing an approach allowing nonzero w' at the lower boundary would be difficult.

[29] Because w' is zero at the model lower boundary the waves cannot be forced there. Instead, the model domain is extended below z = 0 so that the model lower boundary is at z = −1 km and wave forcing is applied at z = −0.5 km by specifying the amplitude of the temperature perturbation in the form of a thin Gaussian with half width 1/8 km. The value of w' that we calculate at z = 0 (1 km above the model boundary) is very nearly the same as the value which, if applied as a model lower boundary condition at z = 0, would force the solution that we obtain for $z > 0$. The results would differ only if there were significant reflection and the location of the model lower boundary significantly altered standing wave behavior. Tests revealed no such sensitivity to changes in the location of the lower boundary.

[30] Five separate waves are simulated, with periods of 1, 2, 3, 4, and 5 min. Wave amplitudes are scaled to give a maximum heating rate of 100 K day^{-1} for the 1-min wave, which corresponds to a maximum volumetric heating rate of 8.17×10^{-11} W m^{-3}. This same value of maximum volumetric heating rate is prescribed for the four remaining waves. The mean state of the atmosphere is the same as that used in the work of *Hickey et al.* [2001].

4. Results

[31] Five runs were performed corresponding to waves with periods of 1–5 min at 1-min intervals. Figures 1 and 2 show the temperature disturbance corresponding to these waves. There is a consistent tendency for the peak amplitude and the altitude of the peak to increase with wave period. The peak amplitude for the 1-min wave is about 6 K at 230 km. There is no definite peak for the 5 min wave; it achieves a maximum temperature above ~350 km where it obtains a value of nearly 40 K. This might seem paradoxical because one normally expects faster waves to reach greater altitudes before they dissipate. The reason the slower waves reach higher altitudes (and thus obtain greater amplitudes) is explained by an examination of the phase. The slower waves have longer vertical scales and this gives a slower dissipation rate. In fact, the 5-min wave is evanescent or near evanescence below about 400 km, since it is not too far from the acoustic cutoff frequency.

[32] We remark that the vertical velocities associated with these waves can be large. At the peak they range from ~10 m s^{-1} (~230 km) for the 1-min wave to ~70 m s^{-1} for the 5-min wave (~450 km). These values are not

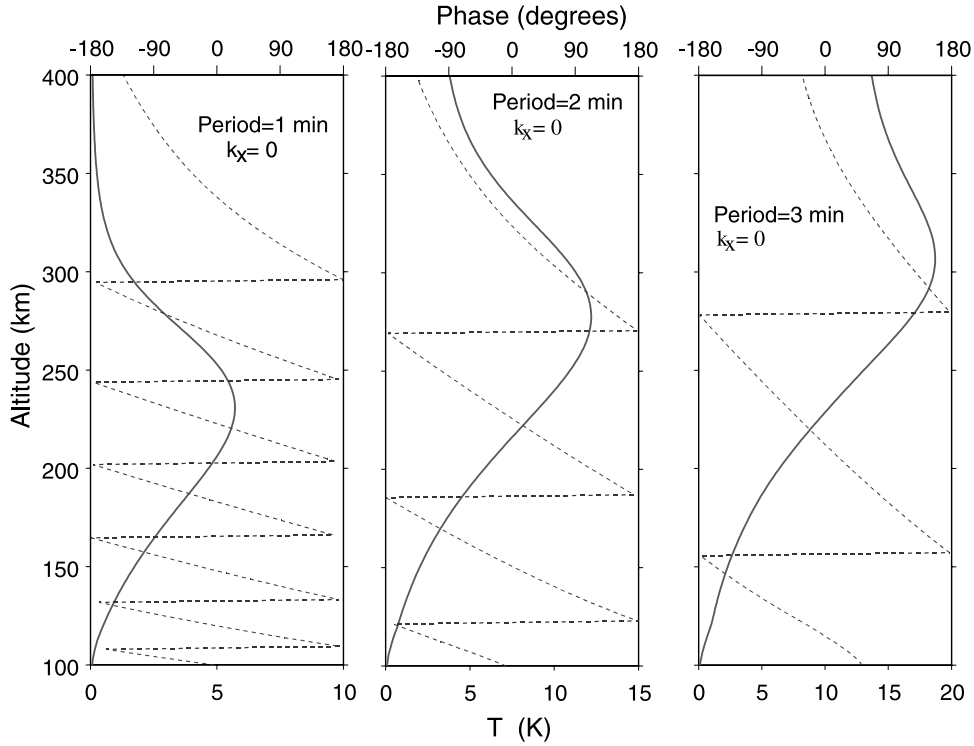

Figure 1. The perturbation temperature amplitude (solid) and phase (dashed) versus altitude for the 1, 2, and 3-min waves. See color version of this figure in the HTML.

unphysical. Vertical velocities greater than 50 m s^{-1} have been measured frequently at red line altitudes, much larger than we predict [*Price et al.*, 1995; *Ishi et al.*, 1999]. The largest predicted vertical winds occur at great heights where the density and the kinetic energy density (or dynamic pressure) are very low. The vertical wind in relation to the vertical phase speed is small and the fractional change in the temperature is small as well, being <1%. This indicates that waves are not subject to instabilities or strong nonlinearities.

[33] Figures 3 and 4 give the heating rates in K day^{-1} for each of the waves shown in the previous figures. The heating rates are shown for various terms in the heat equation. They are described in detail by *Schubert et al.* [2003, 2005]. Briefly, these terms represent the heating rates due to viscous dissipation of wave kinetic energy, Q_{vis}, the sensible heat flux divergence, $Q_{w'T'}$ [*Walterscheid*, 1981], the work done by the wave-induced pressure gradients, $Q_{v'gradp'}$ and the work done by the second-order wave-induced Eulerian drift in transporting mass in the gravitational field, $Q_{w'\rho'}$.

[34] A significant feature of the result is that all terms other than the heat flux divergence exhibit a high degree of cancellation so that the net heating resembles the heat flux divergence. Also, we remark that the effect is to heat the atmosphere, the opposite of what occurs when gravity waves dissipate [*Walterscheid*, 1981]. As for temperature, the net heating increases and peaks at higher altitudes with increasing period, except that the altitudes of the peak heating for the 4 and 5 min waves are nearly the same. By construction, the heating peaks at 100 K day^{-1} at an altitude of 250 km for the 1-min wave. For the 5 min wave the maximum heating is ~1600 K day^{-1} and peaks near 350 km. The results for all waves are given in Table 2.

[35] The heating rates for the slower waves are quite significant. It is interesting to examine the wave forcing associated with these heating rates. From Table 2 it is seen that our approach to normalizing the forcing (producing the same peak volumetric heating rate) has also resulted in essentially the same input energy flux in the lower thermo-

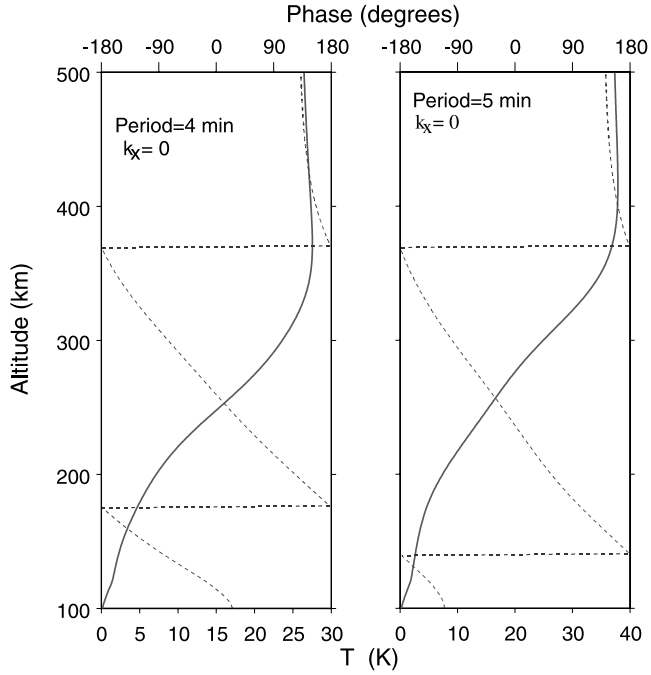

Figure 2. Same as Figure 1 except 4 and 5 min waves. See color version of this figure in the HTML.

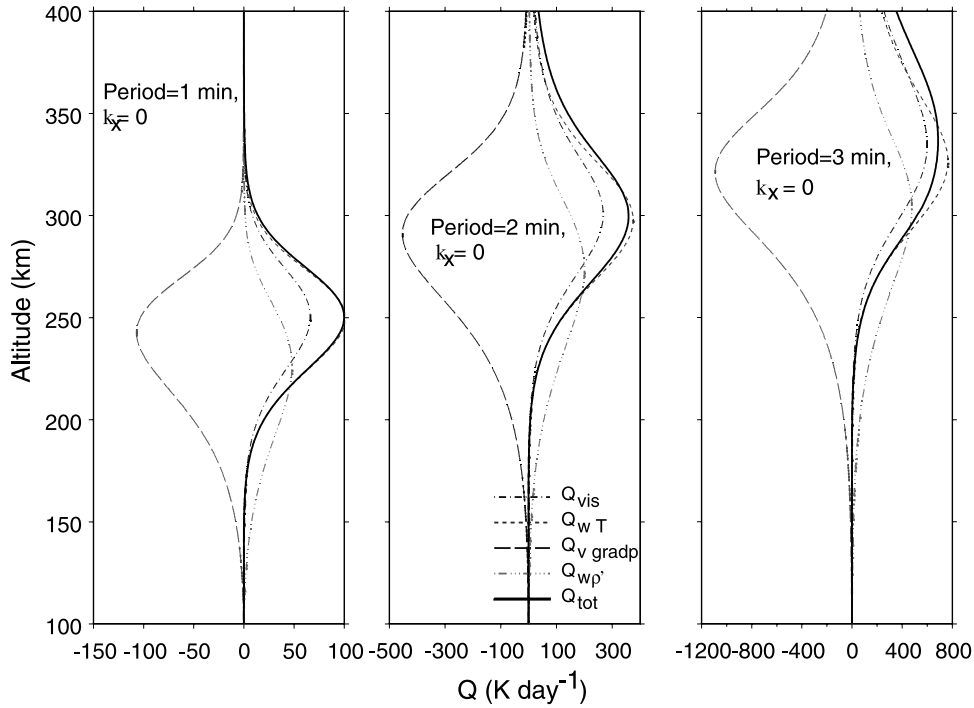

Figure 3. Same as Figure 1 except for heating rates per unit mass in K day^{-1}. The various curves are the total heating and the heating due to various individual processes. The description of the various symbols used and their physical interpretations are given in the text. See color version of this figure in the HTML.

sphere. Thus the differences in per mass heating rate reflect primarily differences in how the heat is distributed vertically, rather than the energy input. It is obvious that very large effects can be produced with weak forcing, especially for the slower waves (period $\geq$3 min).

[36] The steady-state model clearly overstates the heating that would result from a single wave packet. However, if we assume that an extensive region of hilly terrain is a source of more or less constant generation of waves, then we can ask what amplitudes are required to produce significant heating at higher thermospheric altitudes given the heating rates in Table 2. If we assume that 100 K day^{-1} is significant, then we get the results shown in Table 3.

[37] The results shown in Table 3 indicate that a steady flux of waves in the acoustic range can produce significant heating if the vertical velocity forcing is of the order of 10^{-4} m s^{-1}, except for the 5-min wave where much stronger forcing is required. The stronger forcing required for the 5-min wave reflects the evanescence and near evanescence for this wave. However, the results presented in Table 1 and the following discussion indicate that significantly stronger forcing is available for a wave of this frequency.

[38] Tables 2 shows that if the heating is highly episodic (occurring on the order of 10% of the time at a given place), then forcing should generally be on the order of 10^{-3} m s^{-1}. The analysis in the previous section indicates that this would require antisymmetric eddies with timescales $\sim$10 min or less with strengths of $\sim$1 m s^{-1}. The requirement on the vertical velocity is far less stringent if the heating is much less episodic. Then Table 3 indicates that eddy strengths of $\sim 10^{-1}$ m s^{-1} should be sufficient to provide significant heating rates in the thermosphere.

[39] It is interesting to compare the acoustic wave results to fast gravity waves normalized to give the same energy flux as the acoustic waves. We performed simulations for a 10-min gravity wave with a horizontal phase speed of 50 m s^{-1} and for 20-min waves with phase speeds of 50

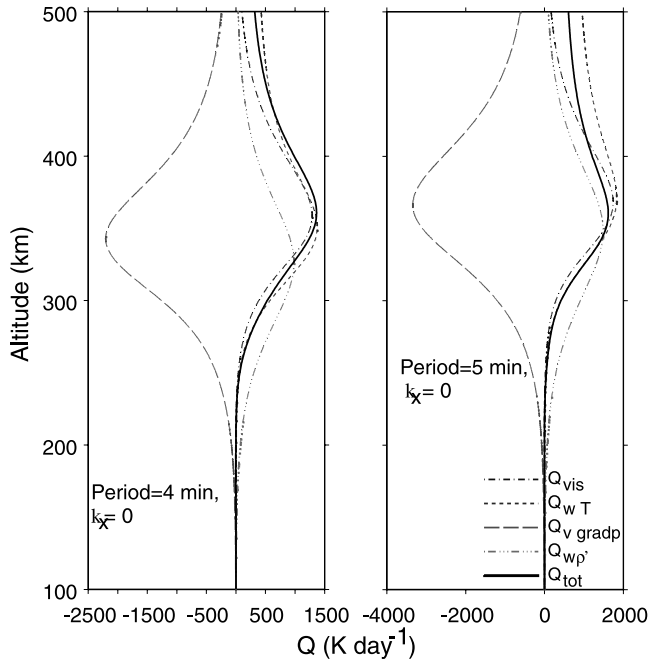

Figure 4. Same as Figure 3 except for 4 and 5 min waves. See color version of this figure in the HTML.

Table 2. Altitude and Value of Peak Heating for the Waves Considered[a]

Period, min	Vertical Wind at $z = 0$, m s^{-1}	F_z at $z = 120.5$ km, W m$^{-2} \times 10^6$	Altitude of Peak Heating, km	Peak Heating Rate, K day^{-1}
1	2.15×10^{-4}	6.13	250	100
2	1.89×10^{-4}	7.11	299	358
3	1.96×10^{-4}	7.69	337	687
4	3.59×10^{-4}	8.96	361	1364
5	6.29×10^{-3}	8.23	360	1618

[a]Also shown are the vertical winds at $z = 0$ and wave energy flux F_z at a model altitude of $z = 120.5$ km.

and 100 m s^{-1}. Evanescence is favored by fast phase speeds and frequencies near the Brunt-Väisälä. The 10-min wave suffered some attenuation due to the latter cause alone, and we did not run this case for the faster phase speed. For all gravity waves we imposed the same energy flux near 120 km as for the acoustic waves ($\sim 7 \times 10^{-6}$ W m^{-2}). The gravity waves induced a downward flux of heat that cooled the thermosphere where heat was extracted and warmed it where heat was deposited. The 10-min wave gave the smallest effects because of the combined effects of viscous dissipation in the lower thermosphere and evanescence above. The thermal effects were largest for the 20-min wave with the 100 m s^{-1} phase speed. The maximum heating was $\sim$6 K day^{-1} near 150 km altitude and the maximum cooling was by $\sim$12 K day^{-1} near 196 km. By redline altitudes cooling dropped to $\sim$1 K day^{-1}. Stronger waves would increase the cooling at redline altitudes but not give heating. This suggests that high-frequency gravity waves generated in the troposphere are an inefficient source of wave heating for the middle thermosphere and above.

5. Discussion and Conclusions

[40] The calculations presented here suggest that over a dense array of geographically extensive sources orographically generated vertically propagating ($k \approx 0$) acoustic waves may be a significant cause of thermospheric heating. Simple theoretical considerations suggest that antisymmetric eddies with durations on the order of 10 min can force waves in the 1 to 5-min range with efficiencies of 10^{-3} to 10^{-4}. The efficiency is measured by the output vertical wind in the wave number-frequency band of interest divided by the input eddy horizontal wind. The larger values apply to the slower waves considered. Depending on the intermittency of wave generation, eddy strengths of order 1 m s^{-1} (10% intermittency) to 0.1 m s^{-1} (nearly constant supply of wave packets) are sufficient to give significant heating.

[41] Measurements often reveal energetic gravity waves in the mesospause region with longer periods and shorter vertical wavelengths than those we have considered. Sodium lidar measurements, for example, show significant disturbances having vertical wavelengths of 10 km to 20 km [e.g., *Gardner and Voelz*, 1987; *Senft and Gardner*, 1991; *Swenson et al.*, 2000]. These waves can exist at mesopause heights because eddy diffusivity is small ($\sim$100 m^2 s^{-1}) and molecular diffusivity is effectively nil. Molecular diffusion increases rapidly with altitude, achieving values of $\sim 10^4$ m^2 s^{-1} at 150 km altitude [e.g., *Hickey et al.*, 2001] and viscous filtering of waves becomes important. *Hines* [1964] derived a simple expression relating the kinematic viscosity to the minimum vertical wavelength required for a gravity wave to avoid severe damping in the thermosphere. His results suggest that gravity waves having vertical wavelengths comparable to those that dominate the spectrum in the upper mesosphere and lower thermosphere should experience strong damping above about 140 km altitude. A similar conclusion was later reached by *Swenson et al.* [1995] using a similar approach. Gravity waves that typically dominate in the mesopause region will therefore be viscously damped in the lower thermosphere and will be unable to propagate into the middle thermosphere and above. These waves are unlikely to play a significant role in the heat budget of the middle and upper thermosphere.

[42] There are many observations revealing gravity waves of lower atmospheric origin propagating near 250 km altitude [e.g., *Bertel et al.*, 1978; *Bertin et al.*, 1978]. These waves typically have phase speeds exceeding 150 m s^{-1} and vertical wavelengths exceeding 90 km. High-frequency waves with these phase speeds and vertical wavelengths would be similar to the waves we have considered above and have shown to be ineffective in heating the thermosphere. Low-frequency waves with similar phase speeds and vertical wavelengths would have to be large-scale waves. There might be significant excitation of such fast moving gravity waves by fairly slow wind variations over larger-scale terrain. To be effective heat sources, these waves have to overcome the depleting effects of geometric spreading as they propagate outward from the source and overcome the cooling effects of vertical heat transport in regions of strong wave damping [*Walterscheid*, 1981; *Walterscheid et al.*, 2001]. However, lower-frequency waves tend to be more energetic, and we cannot rule out significant thermosphere heating from these waves.

[43] It is interesting to consider flow over isolated peaks. For an isolated hill the analog to waves of the form $\exp(ikx)$ with $k \approx 0$ is $J_0(kr)$ with $k \approx 0$, where J_0 is the Bessel function of the first kind of zero-order and r is the radial distance from the axis of the hill [*Walterscheid et al.*, 2001].

Table 3. Approximate Vertical Winds at $z = 0$ Required to Produce a Heating Rate of 100 K day^{-1} at the Altitude of Peak Heating (Also Shown)

Period, min	Altitude of Peak Heating, km	Vertical Wind at $z = 0$, m s^{-1}
1	250	2.15×10^{-4}
2	299	9.99×10^{-5}
3	337	7.46×10^{-5}
4	361	9.71×10^{-5}
5	360	1.56×10^{-3}

For $k \approx 0$, $J_0(kr)$ and $\exp(ikx)$ are both ≈ 1, provided r is not too large; thus for the particular case of $k \approx 0$ the isolated hill is similar to an extended ridge insofar as the behavior directly above the hill is concerned. However, one must account for the fact that the eddy and its interaction with the hill necessarily have a strong azimuthal dependence and only part of the resultant w' will project on J_0. The projection on J_0 may be analyzed by first averaging in azimuth. A reasonable model of the azimuthal dependence of w' is one that varies as the absolute value of a wave number 1 variation. This is one that has its maximum value where the flow is maximally up- or down-slope (0 and 180°, say) and is zero on the flanks (±90°). The azimuthal average of such a variation is $\sim 2/\pi$, which is not too different from unity. Thus for the particular case of vertically propagating waves the three dimensionality of isolated interactions does not radically alter the resulting disturbance obtained by considering interactions involving two dimensional terrain.

[44] For a horizontally extended field of complex terrain, one can relax the restriction on the permissible range of k because the domains of influence of different terrain features can overlap in the thermosphere. Overlapping domains of influence reduce the diminution of wave effects due to horizontal spreading away from the source. For a horizontally extensive array of dense sources a far greater spread of horizontal wave number can be involved. This means that the ~1% efficiency inferred from a narrow band near $k = 0$ becomes a significant underestimate of the efficiency.

[45] We have analyzed one wave at a time. A reasonable decomposition of the forcing is one where the waves are evenly spaced in frequency according to $\omega_n = n\omega_1$, where $\omega_1 = 2\pi/t_G$. For an assumed eddy duration of 10 min we have the sequence of periods 5, 3.3, 2.5, 2.0, 1.67 1.43, 1.25, 1.11, and 1 min in the acoustic range of interest. Referring to the heating rate figures (Figures 3 and 4), we conclude that there is considerable overlap in the heating profiles for the various waves. The collective effects would give heating rates ~2–3 times greater than indicated by individual profiles. Perhaps more importantly, the collective effects can mitigate the diminution of heating by intermittency. Multiwave considerations significantly reinforce indications that orographic effects may be a significant source of acoustic wave heating.

[46] Finally, convection itself might be an even more prolific source of acoustic wave generation over hills than the indirect source due to related changes in the horizontal wind. Convection associated with thunderstorms is known to be a significant source of gravity waves [*Walterscheid et al.*, 2003, and references therein]. Convection associated with hills will produce much less heating than thunderstorm sources, but changes in convection over hills can be more rapid, making them more effective generators of acoustic waves. *Tian and Parker* [2003] simulated the diurnal variation in convection over hills under various wind conditions. In zero wind conditions they found fairly vigorous convection. For a hill of length 10 km and height 500 m they found maximum values of the vertical wind at the summit ~4 m s^{-1}. The buildup and decay each took place over about 4 hours. However, large changes ~1–2 m s^{-1} took place on much shorter timescales within the overall growth and decay. These changes occurred on the timescale of the plotting resolution (30 min), but the high degree of variability at this sampling interval and the very small vertical velocities required to give a large thermospheric response together suggest a significant source of acoustic waves.

[47] We conclude that though the strength and intermittency of acoustic-wave generation by the eddy field are not known, the required amplitudes seem small enough to make orographically acoustic waves a plausible source of significant wave heating. We regard our results as reasonably robust, especially when one considers multiwave and multisource effects for a horizontally extensive array of sources. This heating may account in good part for the thermospheric hot spot near the Andes reported by *Meriwether et al.* [1996, 1997].

[48] **Acknowledgments.** Work by RLW was supported by NASA grant NAG5-13025. MPH was supported by NASA grant NAG5-10251, NSF grant ATM-0242896, and by the Aerospace Corporation through funding received under NASA grant NAG5-13025.

[49] Arthur Richmond thanks John Meriwether and another reviewer for their assistance in evaluating this paper.

References

Agee, E., and A. Gluhovsky (1999), LES model sensitivities to domains, grids, and large-eddy timescales, *J. Atmos. Sci.*, *56*, 599–605.

Allen, T., and A. R. Brown (2002), Large-eddy simulation of turbulent separated flow over rough hills, *Boundary Layer Meteorol.*, *102*, 177–198.

Barndorff-Nielson, O. E., and B. B. Willetts (1991), Aeolian grain transport. II: The erosional environment, *Acta Mech.*, *2*, suppl.

Belcher, S. E., and J. C. R. Hunt (1998), Turbulent flows over hills and waves, *Annu. Rev. Fluid Mech.*, *30*, 507–538.

Bertel, L., F. Bertin, J. Testud, and D. Vidal-Madjar (1978), Evaluation of the vertical flux of energy into the thermosphere from medium scale gravity waves generated by the jet stream, *J. Atmos. Terr. Phys.*, *40*, 691.

Bertin, F., J. Testud, L. Kersley, and P. R. Rees (1978), The meteorological jet stream as a source of medium scale gravity waves in the thermosphere: An experimental study, *J. Atmos. Terr. Phys.*, *40*, 1161.

Carruthers, D. J., and J. C. R. Hunt (1990), Fluid mechanics of airflow over hills: turbulence, fluxes and waves in boundary layer, in *Atmospheric Processes Over Complex Terrain*, *Am. Meteorol. Soc. Monogr.*, chap. 5, Am Meteorol. Soc., Boston.

Gardner, C. S., and D. G. Voelz (1987), Lidar studies of the nighttime sodium layer over Urbana, Illinois. 2. Gravity waves, *J. Geophys. Res.*, *92*, 4673–4694.

Gopalakrishnan, S. G., S. B. Roy, and R. Avissar (2000), An Evaluation of the scale at which topographical features affect the convective boundary layer using large eddy simulations, *J. Atmos. Sci.*, *57*, 334–351.

Grabowski, W. W., and T. L. Clark (1991), Cloud-environment interface instability: rising thermal calculates in two spatial dimensions, *J. Atmos. Sci.*, *48*, 527–546.

Gradshteyn, I. S., and I. M. Ryzhik (1965), *Table of Integrals, Series, and Products*, 1086 pp., Elsevier, New York.

Hecht, J. H., S. K. Ramsay Howat, R. L. Walterscheid, and J. R. Isler (1995), Observations of spectra of intensity fluctuations of the OH Meinel nightglow during ALOHA-93, *Geophys. Res. Lett.*, *22*, 2873–2876.

Hickey, M. P., R. L. Walterscheid, and G. Schubert (2000), Gravity wave heating and cooling in Jupiter's thermosphere, *Icarus*, *148*, 266–281.

Hickey, M. P., G. Schubert, and R. L. Walterscheid (2001), Acoustic wave heating of the thermosphere, *J. Geophys. Res.*, *106*, 21,543–21,548.

Hines, C. O. (1964), Minimum vertical scale sizes in the wind structure above 100 kilometers, *J. Geophys. Res.*, *69*, 2847–2848.

Hocke, K., and T. Tsuda (2001), Gravity waves and ionospheric irregularities over tropical convection zones observed by GPS/MET radio occultation, *Geophys. Res. Lett.*, *28*, 2815–2818.

Ishii, M., S. Oyama, S. Nozawa, R. Fujii, E. Sagawa, S. Watari, and H. Shinagawa (1999), Dynamics of neutral wind in the polar region observed with two Fabry-Perot interferometers, *Earth Planets Space*, *51*, 833–844.

Jones, W. L. (1970), A theory for quasi-periodic oscillations observed in the ionosphere, *J. Atmos. Terr. Phys.*, *32*, 1555–1566.

Lumley, J. L., and H. A. Panofsky (1964), *The Structure of Atmospheric Turbulence*, Interscience, New York.

Mason, P. J., and R. J. Sykes (1979), Flow over isolated hill of moderate slope, *Q. J. R. Meteorol. Soc.*, *105*, 383–395.

Meriwether, J. W., J. L. Mirick, M. A. Biondi, F. A. Herrero, and C. G. Fesen (1996), Evidence for orographic wave heating in the equatorial thermosphere at solar maximum, *Geophys. Res. Lett.*, *23*, 2177–2180.

Meriwether, J. W., M. A. Biondi, F. A. Herraro, C. G. Fesen, and D. C. Hallenback (1997), Optical interferometric studies of the nighttime equatorial thermosphere: Enhanced temperatures and zonal wind gradients, *J. Geophys. Res.*, *102*, 20,041–20,058.

Price, G. D., R. W. Smith, and G. Hernandez (1995), Simultaneous measurements of large vertical winds in the upper and lower thermosphere, *J. Atmos. Terr. Phys.*, *57*, 631.

Prusa, J. M., P. K. Smolarkiewicz, and R. R. Garcia (1996), Propagation and breaking at high altitudes of gravity waves excited by tropospheric forcing, *J. Atmos. Sci.*, *53*, 2186–2216.

Raju, D. G. K., M. S. Rao, B. M. Rao, C. Jogulu, C. P. Rao, and R. Ramanadham (1981), Infrasonic oscillations in the F_2 region associated with severe thunderstorms, *J. Geophys. Res.*, *86*, 5873–5880.

Rastogi, P. K., and S. A. Bowhill (1976), Gravity waves in the equatorial mesosphere, *J. Atmos. Terr. Phys.*, *38*, 51–60.

Redelsperger, J.-L., and T. L. Clark (1990), The initiation and horizontal scale selection of convection over gently sloping terrain, *J. Atmos. Sci.*, *47*, 516–541.

Rind, D. (1978), Investigation of the lower thermosphere results of ten years of continuous observations with natural ultrasound, *J. Atmos. Terr. Phys.*, *40*, 1199–1210.

Schubert, G., M. P. Hickey, and R. L. Walterscheid (2003), Heating of Jupiter's thermosphere by the dissipation of upward propagating acoustic waves, *Icarus*, *163*, 398–413, doi:110.1016/S0019-1035(03)00078-2.

Schubert, G., M. P. Hickey, and R. L. Walterscheid (2005), Physical processes in acoustic wave heating of the thermosphere, *J. Geophys. Res.*, *110*, D07106, doi:10.1029/2004JD005488.

Senft, D. C., and C. S. Gardner (1991), Seasonal variability of gravity wave activity and spectra in the mesopause region at Urbana, *J. Geophys. Res.*, *96*, 17,229–17,264.

Sivjee, G. G., and R. L. Walterscheid (2005), Observations of elevated power near the Brunt-Väisälä frequency, *J. Geophys. Res.*, *110*, A06305, doi:10.1029/2004JA010892.

Solomon, S. C., and V. J. Abreu (1989), The 630 nm dayglow, *J. Geophys. Res.*, *94*, 6817–6824.

Swenson, G. R., C. S. Gardner, and M. J. Taylor (1995), Maximum altitude penetration of atmospheric gravity waves observed during ALOHA-93, *Geophys. Res. Lett.*, *22*, 2857–2860.

Swenson, G. R., M. J. Alexander, and R. Haque (2000), Dispersion imposed limits on atmospheric gravity waves in the mesosphere: Observations from OH airglow, *Geophys. Res. Lett.*, *27*, 875–878.

Takahashi, H., B. R. Clemesha, R. P. Batista, Y. Sahai, M. A. Abdu, and P. Muralikrishna (1990), Equatorial F-region OI 6300 Å and OI 5577 Å emission profiles observed by rocket-borne airglow photometers, *Planet. Space Sci.*, *38*, 547–554.

Taylor, P. A., and H. W. Teunissen (1987), The Askervien hill project: overview and background data, *Boundary Layer Meteorol.*, *39*, 15–39.

Tian, W., and D. J. Parker (2003), A modeling study and scaling analysis of orographic effects on boundary layer shallow convection, *J. Atmos. Sci.*, *60*, 1981–1991.

van der Hoven, I. (1957), Power spectrum of horizontal wind speed in the frequency range from 0.0007 to 900 cycles per hour, *J. Meteorol.*, *14*, 160.

Walterscheid, R. L. (1981), Dynamical cooling induced by dissipating internal gravity waves, *Geophys. Res. Lett.*, *8*, 1235–1238.

Walterscheid, R. L., and J. H. Hecht (2003), A reexamination of evanescent acoustic-gravity waves: special properties and aeronomical significance, *J. Geophys. Res.*, *108*(D11), 4340, doi:10.1029/2002JD002421.

Walterscheid, R. L., G. Schubert, and D. G. Brinkman (2001), Small-scale gravity waves in the upper mesosphere and lower thermosphere generated by deep tropical convection, *J. Geophys. Res.*, *106*, 31,825–31,832.

Walterscheid, R. L., G. Schubert, and D. G. Brinkman (2003), Acoustic waves in the upper mesosphere and lower thermosphere generated by deep tropical convection, *J. Geophys. Res.*, *108*(A11), 1392, doi:10.1029/2003JA010065.

M. P. Hickey, Department of Physical Sciences, Embry Riddle Aeronautical University, Daytona Beach, FL 32114-3900, USA.

R. L. Walterscheid, NOAA/NESDIS at EUMETSAT, Am Kavallriensand 31, D-64295 Darmstadt, Germany. (Richard.Walterscheid@uemetsat.int)